



ChemComm

Tuning Near Infrared II Emitting Wavelength of Small Molecule Dyes by Single Atom Alteration

Journal:	<i>ChemComm</i>
Manuscript ID	CC-COM-10-2019-008434.R1
Article Type:	Communication

SCHOLARONE™
Manuscripts

COMMUNICATION

Tuning Near Infrared II Emitting Wavelength of Small Molecule Dyes by Single Atom Alteration

Received 00th January 20xx,
Accepted 00th January 20xx

Kun Qian,^{a,b} Chunrong Qu,^b Xiangyu Ma,^a Hao Chen,^b Martha Kandawa-Schulz,^c Wei Song,^c Weimin Miao,^d Yihong Wang,^{*a} and Zhen Cheng^{*b}

DOI: 10.1039/x0xx00000x

A series of small molecule dyes demonstrate the feasibility of manipulating Near Infrared II emission by simply altering the donors' heteratoms, which involved both electronegativity and intramolecular steric effect. Furthermore, these dyes show high resolution and stability for *in vivo* imaging after complexed with human serum albumin.

Second near infrared window (NIR-II, 1000-1700 nm) is more appealing for *in vivo* optical imaging since researchers reveal it as "biological transparent",¹ where tissue photon scattering/absorption and bio-autofluorescence are reduced to a relatively low level,² leading to deeper tissue penetration and higher signal contrast compared with visible and first near infrared (NIR-I) optical imaging (400-900 nm).^{3,4}

Several types of NIR-II probes have been reported, including semiconducting polymers, rare earth doped nanoparticles, quantum dots, and single-walled carbon nanotubes, etc.⁵⁻⁹ But these nanoparticles' unclear long-term *in vivo* toxicity, possible heavy ion leakage, and tardy clearance from living subject limit their further development in clinical applications.¹⁰ Small molecule dyes (SMDs) have short-term retention in body, limited bio-toxicity, and biodegradability,¹¹ making them much safer towards living systems and having high potential for clinical translation.

CH1055 is the first reported SMD for NIR-II imaging with strong electron acceptor benzo[1,2-c:4,5-c']bis[1,2,5]thiadiazole (BBTD) to form the classic donor-acceptor-donor (D-A-D) structure.^{5,12} Since then, for even deeper tissue penetration and better imaging clarity, many molecules were designed to have red-shifted emissions by

extending the conjugation backbone. Q4 uses thiophene as bridge between the donor and acceptor of CH1055 to achieve prolonged conjugation backbone and therefore red shifted emission.¹³ Sletten and co-workers successfully prepared a panel of red shifted NIR-II dyes by lengthening the polymethine linker.¹⁴

This strategy is effective but increases structural flexibility and therefore invokes internal conversion decay, leading to lower quantum yield (QY).^{15,16} It also complicates synthesis process and hinders NIR-II SMDs' production in larger scale. Besides, structure modification in such extent may change SMDs' chemical and physical properties, reducing binding efficiency with bio-macromolecules or hampering dye's additional modification. Therefore, to find new and simple methods of tuning emission wavelength in NIR-II window is of great importance.

Materials containing selenophene have showed enhanced charge mobility¹⁷ with lowered band gap (ΔE) between the highest occupied molecular orbital (HOMO) and the lowest unoccupied molecular orbital (LUMO) and promote emission to red shift. On the other hand, decreasing the atomic number of chalcogens in conjugated molecules would shorten the absorption and emission wavelength.¹⁸ Hence, it would be possible to tune the fluorescence wavelength of NIR-II molecules by altering single atom in the conjugation backbone, imposing less effect on other properties of the molecules.

Herein, new NIR-II SMDs (named as FFBA, FTBA, and FSBA, **Figure 1a**) have been designed and synthesized. They share the same structures except donor's chalcogens (O, S, and Se, respectively) to reveal single atom's role in adjusting NIR-II emission wavelength. They were based on s-D-A-D-s (s for shielding unit) structure with BBTD as central acceptor while dialkyl fluorene functioned as the shielding unit. Since the 2-(trimethylsilyl) ethanol residues were far away from the conjugation backbone, their removal would impose limited effect on the emissions and yield FFBA, FTBA, and FSBA. The carboxyl groups of these structures might improve the dye's aqueous solubilities for *in vivo* imaging and could be used for further modification, such as

^a School of Chemistry and Chemical Engineering, Southeast University, Nanjing, 211189, China. Email: yihongwang@seu.edu.cn

^b Molecular Imaging Program at Stanford (MIPS), Bio-X Program, and Department of Radiology, Canary Center at Stanford for Cancer Early Detection, Stanford University, California, 94305-5344, USA. Email: zcheng@stanford.edu

^c Department of Chemistry and Biochemistry, University of Namibia, Windhoek, Namibia

^d Jiangsu Meizhong Medical Technology Co., Ltd. Nantong, China.

Electronic Supplementary Information (ESI) available. See DOI: 10.1039/x0xx00000x

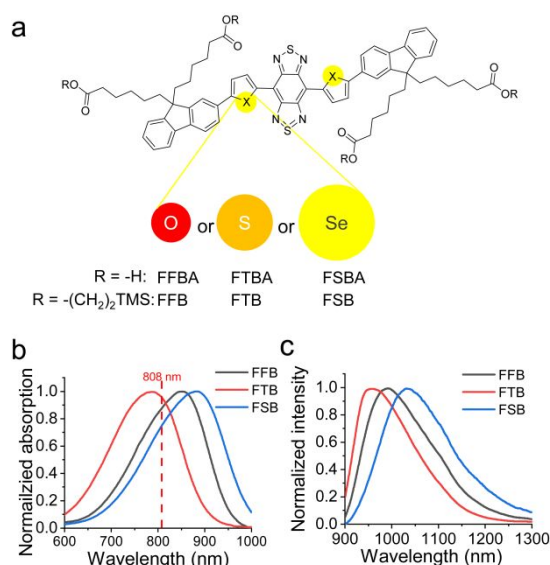


Figure 1. (a) Molecular structure of designed NIR-II fluorophores. (TMS: trimethylsilyl group) Normalized absorption (b) and emission (c) spectra of FFB, FTB, and FSB in toluene. The excitation wavelength was 808 nm as indicated in b (red dash line).

targeting moiety coupling and therapeutic group loading. Matrix-assisted laser desorption/ionization time of flight mass spectra (MALDI-TOF MS) and nuclear magnetic resonance (NMR) spectra (including ¹H NMR and ¹³C NMR) confirmed the successful preparation of the molecules. Detailed synthesis steps and characterization data/spectra can be found in the Electronic Supplementary Information (ESI).

As shown in **Figure 1b**, FTB had the shortest absorption peak at 787 nm while the other two, FFB and FSB, peaked at 850 nm and 884 nm, respectively. These molecules' extinction coefficients at 808 nm, the excitation wavelength, were determined to be 6.9 (FSB), 8.6 (FFB), and 9.9 (FTB) in toluene (unit: $\times 10^3 \text{ L mol}^{-1} \text{ cm}^{-1}$). Their relative QYs were calculated (IR26 as the reference, $\text{QY}_{\text{IR26}} \sim 0.05\%^{19}$) and in the following order: FSB (0.55%) < FFB (0.70%) < FTB (0.79%). Heavy atom effect of Se would increase the singlet-triplet (S-T) conversion process and result in more non-radiative decay,²⁰ partially accounting for the dimmest QY of FSB. According to electronegativity, oxygen atoms from the furan of FFB have the strongest electronic binding ability and should lead to wider band gap and bluer emitting light than those of FTB. However, the emission spectra in **Figure 1c** showed a red shifted emission of FFB (991 nm) relative to FTB (958 nm).

To reveal the possible mechanism of the unanticipated red-shift, density functional theory (DFT) and time-dependent DFT (TDDFT) calculations were proceeded with B3LYP/6-31G(d) scrf method. The graphic presentation of LUMOs in **Figure 2a** and their quantified distribution (Multiwfn, **Table S1**)²¹ show that the LUMOs mainly localized around BBTB cores while FFB had the largest portion there (73.0%) and FSB had the smallest (71.3%), consistent with their donors' ability in restraining electronic mobility. As more extended LUMO would lower energy levels, calculated E_{LUMO} decreased accordingly. Besides, the prolonged LUMO of FSB might increase the intermolecular

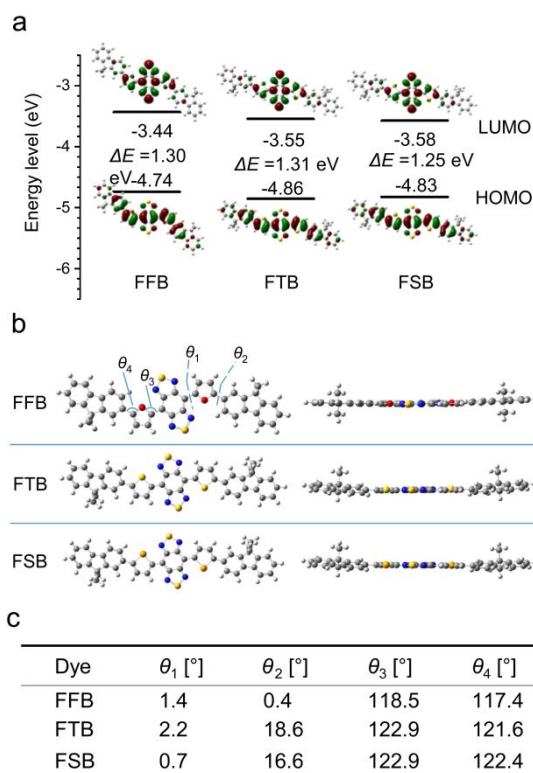


Figure 2. (a) Graphic presentation, energy levels and ΔE of synthesized dyes' HOMO/LUMOs at ground state S_0 , and (b) corresponding optimized geometries (front view and top view). (c) Specific values of the dihedral and plane angles as marked in b.

interaction and lead to lower QY. E_{HOMO} of FTB and FSB increased with atomic numbers and considering their decreasing E_{LUMO} , ΔE_{FTB} was larger than ΔE_{FSB} . However, FFB had the highest HOMO energy level and yielded a smaller ΔE and therefore longer emission wavelength than that of FTB.

Optimized geometries of ground state S_0 (**Figure 2b**) were then evaluated to find clues about FFB's unexpected high E_{HOMO} and red-shifted emission. ϑ_1 and ϑ_2 are the dihedral angles of acceptor-donor and donor-shielding unit planes, respectively, and describe the distortion of the structures. ϑ_3 and ϑ_4 profile the structural stretch extent. Two aspects might affect spatial configuration: intramolecular steric effect and electron delocalization, both following the minimum energy principle. $\vartheta_{2\text{FFB}}$ is much smaller than $\vartheta_{2\text{FTB}}$ and $\vartheta_{2\text{FSB}}$, while $\vartheta_{1\text{FFB}}$ was similar with $\vartheta_{1\text{FTB}}$ and $\vartheta_{1\text{FSB}}$ (**Figure 2c**), indicating FFB had the least distorted S_0 structure, a result of oxygen's smaller atomic size and therefore less intramolecular steric hindrance, which could increase energy level of delocalized HOMO and therefore smaller ΔE . Plane angle ϑ_4 of FTB and FSB were apparently increased by their donor's chalcogens-carbon bond lengths (r), escalating the spatial steric effect. Therefore, increases of $\vartheta_{2\text{FTB}}$ and $\vartheta_{2\text{FSB}}$ would reduce such effect.²² For longer $r_{\text{Se-C}}$, FSB should be more twisted than FTB, but its more delocalized HOMO caused by selenium's weaker electronic binding ability could reduce the structure tension and resulted in FSB's smaller ϑ_1 and ϑ_2 than FTB.²³ As shielding units only took up <8% of the LUMOs, impact of larger ϑ_2 on E_{LUMO} was limited. For S_1

geometry (**Figure S1**), all the dihedral angles decreased for the planarization of π conjugation when excited.

We then tried to apply these probes to in vivo imaging, but once dispersed in phosphate buffer saline (PBS), their fluorescence became very dim (**Figure 3a**, left tubes) because of water molecules' quenching effect,²⁴ making them unsuitable for imaging applications. Their solubility was also limited. Therefore, a biocompatible vehicle able to keep water away from SMDs and soluble in water would be favored.^{25,26}

Endogenous human serum albumin (HSA) was selected as the vehicle for its natural hydrophobic binding cavity and good aqueous solubility.²⁷ Molecular docking results (**Figure S2**) show that these SMDs fit well in the docking sites and there is enough space for the binding without affecting HSA's structure. Several polar contacts between the protein and SMDs are also observed and would benefit the dye-protein complex formation. The docking cavities are in the well-known hydrophobic pocket of HSA, which could exclude water around docked dyes, avoid intermolecular interaction, and therefore enhance their fluorescent intensities.²⁸⁻³⁰

Binding FFBA, FTBA, and FSBA with HSA increased their aqueous fluorescence from almost none to observable, and after heated for 10 min, these complexes showed bright emission (**Figure 3a, b**). Heating HSA appropriately would unfold its structure without damaging the protein permanently and expose the inner hydrophobic binding sites for small molecules.³¹ The optimal molar ratio of dyes/HSA and heating temperature were found to be 2:1 and 50°C for better fluorescence enhancement (**Figure S3a, b**). Compared with emission spectra in toluene, the binding had little impact on the emission spectra with slight blue shift (**Figure S3c**), verifying the hydrophobicity of the binding cavity. These SMD@HSAs are quite stable in PBS and fetal bovine serum (FBS) with continuous excitation for 120 min (**Figure S4**), better than FDA approved NIR dye ICG.³² No obvious cytotoxicity is observed after normal cell line NIH/3T3 incubated with these complexes at concentrations up to 60 μM for three days (**Figure S5**). Usually

the applied concentrations of probes for in vivo imaging are lower than this.³³

These complexes were then administered in vivo by intravenous injection. Left column of **Figure 3c** was taken with 1000 nm long pass (1000LP) filter before cameras, and all images still showed high photon signals all over the body, generating poor signal to background ratio (SBR) and interfering the extraction of valid information. The fluorescence of our dyes above 1150 nm was lower than that above 1000 nm, but once 1150LP filter was applied, the obtained images still had sufficient signal intensities (**Figure 3c**, right column) for their high QYs and all images became clearer. Blood vessels, especially for FSBA@HSA group, could be clearly seen as longer wavelength results in less tissue scattering and absorption.³⁴ Regions around livers emitted massive signals, implying hepatic excretion was the main metabolic pathway and this was confirmed by ex vivo imaging (**Figure S6**). Hind limbs were then focused to avoid the intense liver signals (**Figure 3d, S7**), and the veins were more obvious when 1150LP was applied. Other filters were also tried to find the optimal filter by comparing the SBRs of resulting images (**Figure S8**). The 1150LP filter had the best contrast for all three dyes and FSBA@HSA showed the highest SBR for its longer emission wavelength. Under 1200LP filter, SBRs dropped dramatically for these SMDs' faint fluorescence above 1200 nm.

As FFBA@HSA could provide better SBR than FTBA@HSA under 1150LP and more luminous fluorescence than FSBA@HSA, we tried it in lymphatic imaging for deeper tissue penetration. 20 min after dye administration through hind paw intradermal (i.d.) injection, two main lymph nodes, namely popliteal and sacral, already emitted intense NIR-II signals (**Figure 3e, S9**). And the SBRs were 6.4 and 5.2, respectively, implying fast accumulation of FFBA@HSA. Four collateral lymph vessels could be easily observed near ankle (**Figure 3f**) and cross section fluorescence intensity profile (**Figure 3g**) showed four peaks correspondingly, while only one or two vessels in the same region were observed in previous works.³⁵ The full widths

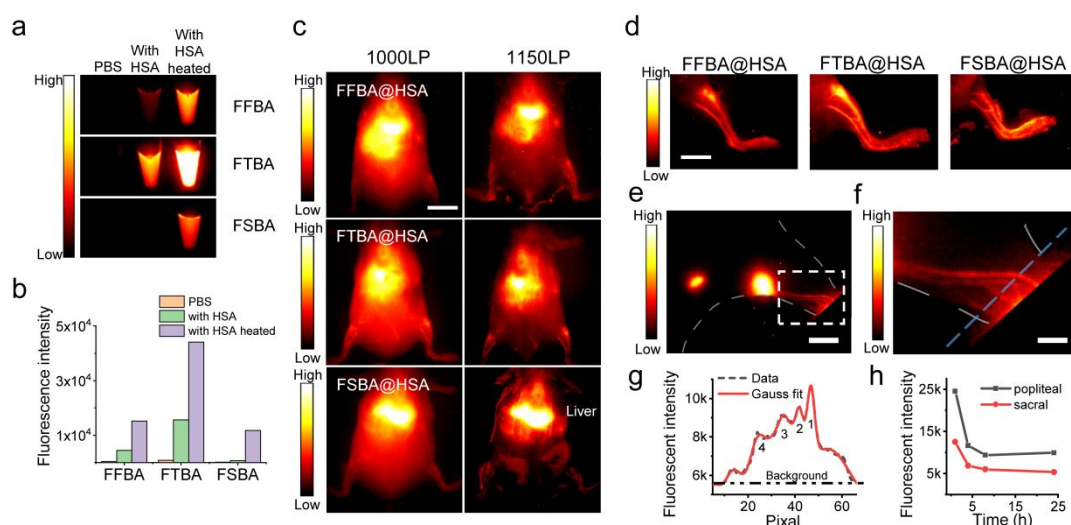


Figure 3. (a) NIR-II imaging and (b) corresponding quantified fluorescence intensities of tubes containing FFBA/FTBA/FSBA in PBS, with HSA in PBS before and after heated at 50°C for 10 min. All samples are tested with 1000LP filter. (c) Whole body (scale bar: 10 mm, 1000LP and 1150LP) and (d) hind limb vascular imaging (scale bar: 5 mm, 1150LP) of C57BL 5 min after intravenous injection of FFBA@HSA, FTBA@HSA and FSBA@HSA. (e) Lymphatic imaging of nude mice 20 min after the intradermal injection of FFBA@HSA (scale bar: 3 mm), and the region of interest (rectangle in white dots) was magnified as in (f) (scale bar: 1 mm). (g) Cross-sectional fluorescent intensity profile (black dash) of the blue dash line in f and its Gaussian fit (red line). (h) Fluorescent signal intensities of the two lymph nodes at different time points.

at half maximum of the four peaks were 400.4, 514.9, 559.2, and 1051.1 μm , demonstrating high spatial resolution. The probe also showed high in vivo stability as the signal intensities from these lymph nodes became steady 4 h later and lasted for more than 24 h (Figure 3h, S10).

In summary, FFB, FTB, and FSB have been successfully prepared with good QYs and demonstrate the feasibility of tuning emission wavelength by single atom altering of NIR-II SMDs. The emission could be affected not only by electronegativity of donor's heteroatom but also by structure distortion extent, which should be considered for future SMDs design. As thiophenes have been widely adopted as donors in NIR-II dyes, this strategy could be easily applied to most of previously reported organic dyes to obtain molecules with different emission wavelength and meet various needs in medical imaging.

HSA greatly enhances the aqueous fluorescence intensities of FFBA, FTBA, and FSBA with decent SBR, high spatial resolution, and good in vivo stability and performance, showing our newly designed dyes' good potential in NIR-II optical imaging.

This work was supported by the Office of Science (BER), U.S. Department of Energy (DE-SC0008397) (ZC), National Natural Science Foundation of China (81571812), Priority Academic Program Development of Jiangsu Higher Education Institutions (1107047002) and Scientific Research Foundation of Graduated School of Southeast University (YBJJ1787).

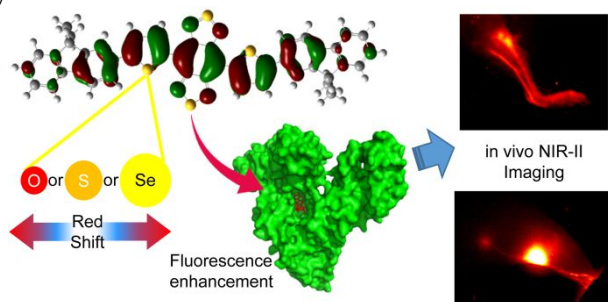
Conflicts of interest

There are no conflicts to declare.

Notes and references

- J. Zhao, D. Zhong and S. Zhou, *J. Mater. Chem. B*, 2018, **6**, 349-365.
- S. He, J. Song, J. Qu and Z. Cheng, *Chem. Soc. Rev.*, 2018, **47**, 4258-4278.
- S. Johnsen, *Biol. Bull.*, 2001, **201**, 301-318.
- J.V. Frangioni, *Curr. Opin. Chem. Biol.*, 2003, **7**, 626-634.
- A.L. Antaris, H. Chen, K. Cheng, Y. Sun, G. Hong, C. Qu, S. Diao, Z. Deng, X. Hu, B. Zhang, X. Zhang, O.K. Yaghi, Z.R. Alamparambil, X. Hong, Z. Cheng and H. Dai, *Nat. Mater.*, 2015, **15**, 235-242.
- C. Liu, K. Wang, X. Gong and A.J. Heeger, *Chem. Soc. Rev.*, 2016, **45**, 4825-4846.
- T. Yang, Y.A. Tang, L. Liu, X. Lv, Q. Wang, H. Ke, Y. Deng, H. Yang, X. Yang, G. Liu, Y. Zhao and H. Chen, *ACS Nano*, 2017, **11**, 1848-1857.
- G. Hong, J.C. Lee, J.T. Robinson, U. Raaz, L. Xie, N.F. Huang, J.P. Cooke and H. Dai, *Nat. Med.*, 2012, **18**, 1841-1846.
- Y. Cao, J. Dou, N. Zhao, S. Zhang, Y. Zheng, J. Zhang, J. Wang, J. Pei and Y. Wang, *Chem. Mater.*, 2017, **29**, 718-725.
- T. Li, C. Li, Z. Ruan, P. Xu, X. Yang, P. Yuan, Q. Wang and L. Yan, *ACS Nano*, 2019, **13**, 3691-3702.
- Q. Yang, Z. Ma, H. Wang, B. Zhou, S. Zhu, Y. Zhong, J. Wang, H. Wan, A. Antaris, R. Ma, X. Zhang, J. Yang, X. Zhang, H. Sun, W. Liu, Y. Liang and H. Dai, *Adv. Mater.*, 2017, **29**, 1605497.
- G. Qian, B. Dai, M. Luo, D. Yu, J. Zhan, Z. Zhang, D. Ma and Z.Y. Wang, *Chem. Mater.*, 2008, **20**, 6208-6216.
- Y. Sun, C. Qu, H. Chen, M. He, C. Tang, K. Shou, S. Hong, M. Yang, Y. Jiang, B. Ding, Y. Xiao, L. Xing, X. Hong and Z. Cheng, *Chem. Sci.*, 2016, **7**, 6203-6207.
- E.D. Cosco, J.R. Caram, O.T. Bruns, D. Franke, R.A. Day, E.P. Farr, M.G. Bawendi and E.M. Sletten, *Angew. Chem. Int. Ed.*, 2017, **56**, 13126-13129.
- Q. Peng, Y. Yi, Z. Shuai and J. Shao, *J. Am. Chem. Soc.*, 2007, **129**, 9333-9339.
- M. Cooper, A. Ebner, M. Briggs, M. Burrows, N. Gardner, R. Richardson and R. West, *J. Fluoresc.*, 2004, **14**, 145-150.
- H. Chen, S. Yeh, C. Chen and C. Chen, *J. Mater. Chem.*, 2012, **22**, 21549.
- M.R. Detty and B.J. Murray, *J. Org. Chem.*, 1982, **47**, 5235-5239.
- C. Qu, Y. Xiao, H. Zhou, B. Ding, A. Li, J. Lin, X. Zeng, H. Chen, K. Qian, X. Zhang, W. Fang, J. Wu, Z. Deng, Z. Cheng and X. Hong, *Adv. Opt. Mater.*, 2019, 1900229.
- J.C. Koziar and D.O. Cowan, *Accounts Chem. Res.*, 1978, **11**, 334-341.
- T. Lu and F. Chen, *J. Comput. Chem.*, 2012, **33**, 580-592.
- J. Lee, M. Kim, B. Kang, S.B. Jo, H.G. Kim, J. Shin and K. Cho, *Adv. Energy Mater.*, 2014, **4**, 1400087.
- M.T. Miller, P.K. Gantzel and T.B. Karpishin, *Inorg. Chem.*, 1999, **38**, 3414-3422.
- C. Yang, X. Wang, S. Huang and M. Wang, *Adv. Funct. Mater.*, 2018, **28**, 1705226.
- Q. Chen and Z. Liu, *Adv. Mater.*, 2016, **28**, 10557-10566.
- S. Wu, Q. Cao, X. Wang, K. Cheng and Z. Cheng, *Chem. Commun.*, 2014, **50**, 8919-8922.
- Z. Liu and X. Chen, *Chem. Soc. Rev.*, 2016, **45**, 1432-1456.
- I. Petitpas, A.A. Bhattacharya, S. Twine, M. East and S. Curry, *J. Biol. Chem.*, 2001, **276**, 22804-22809.
- S. Singha, D. Kim, B. Roy, S. Sambasivan, H. Moon, A.S. Rao, J.Y. Kim, T. Joo, J.W. Park, Y.M. Rhee, T. Wang, K.H. Kim, Y.H. Shin, J. Jung and K.H. Ahn, *Chem. Sci.*, 2015, **6**, 4335-4342.
- K. Qian, H. Chen, C. Qu, J. Qi, B. Du, T. Ko, Z. Xiang, M. Kandawa-Schulz, Y. Wang and Z. Cheng, *Nanomed.-Nanotechnol. Biol. Med.*, 2020, **23**, 102087.
- A.L. Antaris, H. Chen, S. Diao, Z. Ma, Z. Zhang, S. Zhu, J. Wang, A.X. Lozano, Q. Fan, L. Chew, M. Zhu, K. Cheng, X. Hong, H. Dai and Z. Cheng, *Nat. Commun.*, 2017, **8**, 15269.
- M.L.J. Landsman, G. Kwant, G.A. Mook and W.G. Zijlstra, *J. Appl. Physiol.*, 1976, **40**, 575-583.
- C. Martelli, A. Lo Dico, C. Diceglie, G. Lucignani and L. Ottobri, *Oncotarget*, 2016, **7**, 48753-48787.
- S. Zhu, Z. Hu, R. Tian, B.C. Yung, Q. Yang, S. Zhao, D.O. Kiesewetter, G. Niu, H. Sun, A.L. Antaris and X. Chen, *Adv. Mater.*, 2018, **30**, 1802546.
- K. Shou, C. Qu, Y. Sun, H. Chen, S. Chen, L. Zhang, H. Xu, X. Hong, A. Yu and Z. Cheng, *Adv. Funct. Mater.*, 2017, **27**, 1700995.

Table of Contents entry



Replacing donors' S by O and Se will red shift NIR-II dyes' fluorescence emission and offer good clarity/brightness for imaging.